IEEE Access
Multidisciplinary | Rapid Review | Open Access Journal

Received September 9, 2019, accepted October 9, 2019, date of publication October 14, 2019, date of current version October 25, 2019.

Digital Object Identifier 10.1109/ACCESS.2019.2947254

Polar-Coded GFDM Systems

YAN LI, (Student Member, IEEE), KAI NIU, (Member, IEEE), AND CHAO DONG, (Member, IEEE)

Key Laboratory of Universal Wireless Communications, Ministry of Education, Beijing University of Posts and Telecommunications, Beijing 100876, China

Corresponding author: Kai Niu (niukai@bupt.edu.cn)

This work was supported in part by the National Key Research and Development Program of China under Grant 2018YFE0205501, in part by the BUPT Excellent Ph.D. Students Foundation under Grant XTCX201801, and in part by the National Natural Science Foundation of China under Grant 61671080.

ABSTRACT Generalized frequency division multiplexing (GFDM) is a block-based non-orthogonal multi-carrier modulation scheme proposed for 5G PHY layer. In this paper, to efficiently coordinate the features of interference existing in the GFDM system, we propose a theoretical framework of the polar-coded GFDM (PC-GFDM) system, which allows jointly optimizing the combination of binary polar coding and GFDM modulation. The original GFDM channel is decomposed into multiple bit polarized channels by using a two-stage channel transform. The general modulation partition is performed in the first stage and the bit polarization transform is done in the second stage. Specifically, two schemes are considered for the first stage channel transform, multilevel coding (MLC) and bit-interleaved coded modulation (BICM). Based on the theorem we have proved in this paper that the capacities of channels corresponding to all transmitted symbols are identical, the MLC based PC-GFDM system is designed to optimize the combining of polar codes and GFDM system. Then the BICM based PC-GFDM system is designed to reduce the complexity and processing latency, which yields the suboptimal performance. Simulation results indicate that the proposed PC-GFDM systems significantly outperform the existing turbo-coded GFDM systems because of the joint design between the polar coding and the GFDM modulation.

INDEX TERMS Polar codes, GFDM modulation, two-stage channel transform, BICM, MLC.

I. INTRODUCTION

Polar codes proposed by Arıkan [1] are the first constructive codes that have been proved to achieve the symmetric capacity for the binary-input memoryless channels (BMCs). This capacity-achieving code family is based on a technique named channel polarization, which recently has been employed in many scenarios for signal processing. In 2013, Seidl *et al.* have introduced the channel polarization idea into the 2^m-ary modulation scheme [2] and proposed two different polar-coded modulation (PCM) schemes, where the bit-interleaved coded modulation (BICM) [3] and multilevel coding (MLC) approaches are considered respectively. Later, by extending the channel polarization idea to non-orthogonal multiple access (NOMA) scenario, whereby the original NOMA channel is split into a set of binary-input channels under a three-stage channel transform, Dai *et al* design a polar-coded NOMA system [4] to jointly optimize the combination of binary polar coding, signal modulation and NOMA transmission. Similarly, polar-coded multiple-input multiple-output (MIMO) schemes [5] also have been developed to improve the system performance.

Generalized frequency division multiplexing (GFDM) [6], [7] is a flexible non-orthogonal multicarrier modulation scheme proposed for the 5G physical layer. Benefiting from its time-frequency block-based modulation structure, GFDM exhibits several advantages over the orthogonal frequency division multiplexing (OFDM), such as higher spectral efficiency, lower out-of-band (OOB) emission and its flexibility of system configurations, etc. In GFDM, each data block occupying a number of subcarriers and subsymbols is modulated to obtain the transmitted symbols, where the number of subcarriers and subsymbols can be configured flexibly. To reduce the OOB emission, the subcarriers in each block are filtered with a set of pulse shapes, which are circularly shifted versions of a well-localized prototype filter in time and frequency domain. However, the pulse shaping leads to self-interference existing in the transmitted symbols of the GFDM system, which causes the degradation of system performance. Therefore, LTE turbo codes have been used in

The associate editor coordinating the review of this manuscript and approving it for publication was Zesong Fei.

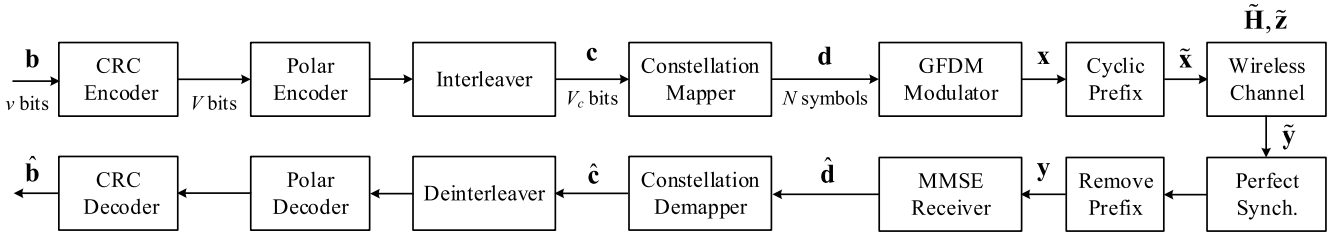

FIGURE 1. Block diagram of GFDM system.

GFDM system to enhance the error performance, which is named as turbo-coded GFDM (TC-GFDM) [8].

In this paper, to compensate for the performance loss caused by the inherent interference, the GFDM system is handled by using the channel polarization. Inspired by the channel-aware feature of polar coding [1] and the generalized channel polarization idea [2], we design the theoretical framework of polar-coded GFDM (PC-GFDM) system based on the two-stage channel transform. By performing the general modulation partition, the GFDM channel is decomposed into a series of binary-input GFDM synthesized channels in the first stage, then the bit polarization transform is performed to obtain a group of bit polarized channels in the second stage. Compared to the TC-GFDM system, the PC-GFDM system jointly optimizes the combination of binary polar coding and GFDM transmission. Under this joint design framework, two PC-GFDM schemes, namely, MLC-PC-GFDM and BICM-PC-GFDM are proposed. First, we have proved that the capacities of channels corresponding to all transmitted symbols are identical, thus the MLC-PC-GFDM is designed to achieve the optimal performance, where the GFDM channel is serially split into a group of correlated binary-input channels in the first stage channel transform. Then to reduce the complexity and processing latency, the BICM-PC-GFDM scheme is designed with the help of an interleaver, where the GFDM channel is parallel divided into a series of independent binary-input channels in the first stage channel transform. At the second stage channel transform, the conventional binary channel polarization is performed for both PC-GFDM schemes.

Through the two-stage channel transform, a series of bit polarized channels will be finally obtained, which exhibit an obvious polarization effect, i.e., tend to be completely either noiseless or noisy. Since the features of interference are efficiently coordinated, the proposed BICM-PC-GFDM system can yield notable performance gains against the conventional TC-GFDM system, which is verified via simulation. Moreover, the MLC-PC-GFDM can further achieve better performance than the BICM-PC-GFDM since there is no loss of mutual information in the MLC scheme.

The remaining sections of the paper are organized as follows. Section II presents the notation conventions and the system model of GFDM. In Section III, the frameworks of the two-stage channel transform under the MLC and BICM modes are described, respectively. The construction procedures of the PC-GFDM systems are provided in Section IV, followed by performance and complexity evaluation for two different channels in Section V. Finally, conclusions are drawn in Section VI.

II. NOTATIONS AND SYSTEM MODEL

A. NOTATION CONVENTIONS

In this paper, the calligraphic letters, such as $\mathcal{X}$ and $\mathcal{Y}$, are used to denote sets and $|\mathcal{X}|$ denotes the cardinality of $\mathcal{X}$. The bold uppercase letters, such as $\mathbf{X}$, stand for matrices and $\mathbf{X}_{i,j}$ denotes the element of i-th row and j-th column of matrix $\mathbf{X}$. We use bold lowercase letters, e.g. $\mathbf{x}$, to denote vectors and use x_i to represent the i-th element in $\mathbf{x}$. The notations $\mathbf{X}^H$ and $\mathbf{x}^H$ denote the conjugate transpose of matrix $\mathbf{X}$ and vector $\mathbf{x}$, respectively. And the notation $\mathbf{x}^T$ stands for the transpose of vector $\mathbf{x}$. The modulus of a complex number x is expressed as $\|x\| = \sqrt{\Re(x)^2 + \Im(x)^2}$, where $\Re(x)$ and $\Im(x)$ denote the real and imaginary parts of x, respectively. In addition, the hollow symbols $\mathbb{B}$, $\mathbb{R}$ and $\mathbb{C}$ are utilized to denote the set of binary, real and complex numbers, respectively. Throughout this paper, $\log(\cdot)$ denotes "logarithm to base 2", and $\ln(\cdot)$ represents the natural logarithm.

B. GFDM SYSTEM MODEL

Fig. 1 depicts the block diagram of the GFDM transceiver, which consists of the following six steps.

Step 1): A data source produces a binary information vector $\mathbf{b}$, whose length is denoted by v, Then a vector of length $V = v + r$ is obtained through the cyclic redundancy check (CRC) encoder, where r is the length of the CRC sequence. The concatenation with CRC aims to assist the SCL decoding to reduce the wrong paths.

Step 2): The coded vector denoted by $\mathbf{c}$ is obtained through polar encoder and interleaver. The length of $\mathbf{c}$ is denoted by V_c and whereby the code rate is expressed as $R = \frac{V}{V_c}$.

Step 3): The complex-valued symbol vector $\mathbf{d}$ of length N is obtained through the constellation modulation, which can be located on K subcarriers and M subsymbols, i.e., the vector $\mathbf{d}$ can be expressed

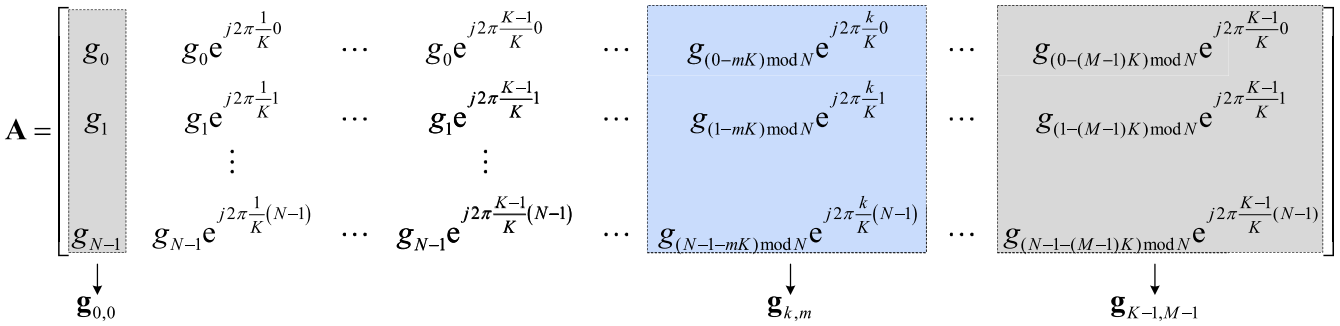

FIGURE 2. The structure of the GFDM modulation matrix A.

as $\mathbf{d} = \left(d_{0,0}, \cdots d_{K-1,0}, d_{0,1}, \cdots, d_{K-1,M-1}\right)$ and thus $N = KM$. Each pair of k-th subcarrier and m-th subsymbol is used to transmit one data symbol $d_{k,m}$ with the corresponding pulse shaping filter $\mathbf{g}_{k,m} = (g_{k,m}[n])^T$ and

$$g_{k,m}[n] = g[(n - mK) \bmod N] \cdot \exp[j2\pi \frac{k}{K} n], \qquad (1)$$

where $k = 0, 1, \cdots, K-1$, $m = 0, 1, \cdots, M-1$ and $n = 0, 1, \cdots, N-1$. Each $\mathbf{g}_{k,m}$ is a time and frequency shifted version of a prototype filter $\mathbf{g} = (g[n])^T$. Hence, the transmit signal $\mathbf{x} = (x[n])^T$ is obtained by superposition of all transmit data symbols as

$$x[n] = \sum_{k=0}^{K-1} \sum_{m=0}^{M-1} g_{k,m}[n] d_{k,m}, n = 0, 1, \cdots, N-1. \qquad (2)$$

Collect all pulse shapes in an $N \times N$ matrix as [6]

$$\mathbf{A} = (\mathbf{g}_{0,0}, \cdots, \mathbf{g}_{K-1,0}, \mathbf{g}_{0,1}, \cdots, \mathbf{g}_{K-1,M-1}), \qquad (3)$$

which is named as the GFDM modulation matrix and whose detailed structure is depicted in Fig. 2. Specifically, when the raised cosine (RC) filter with roll-off factor $\alpha = 0.1$ is adopted as the prototype filter, the time and frequency spectrograph of GFDM is presented in Fig. 3. Thus (2) can be reformulated as a matrix form

$$\mathbf{x} = \mathbf{A}\mathbf{d}. \qquad (4)$$

Then, to avoid interference between subsequent GFDM blocks, a cyclic prefix (CP) contains N_{CP} samples is added to $\mathbf{x}$ to produce the GFDM signal $\tilde{\mathbf{x}}$.

Step 4): Transmission through a wireless channel with impulse response $\mathbf{h} = (h_1, \cdots, h_{N_{ch}})^T$ of length N_{ch} is modeled by

$$\tilde{\mathbf{y}} = \tilde{\mathbf{H}}\tilde{\mathbf{x}} + \tilde{\mathbf{z}}, \qquad (5)$$

where $\tilde{\mathbf{y}}$ is the received signal, $\tilde{\mathbf{z}} \sim \mathcal{CN}(0, \sigma_z^2 \mathbf{I}_{N+N_{CP}+N_{ch}-1})$ denotes the additive white Gaussian noise (AWGN),

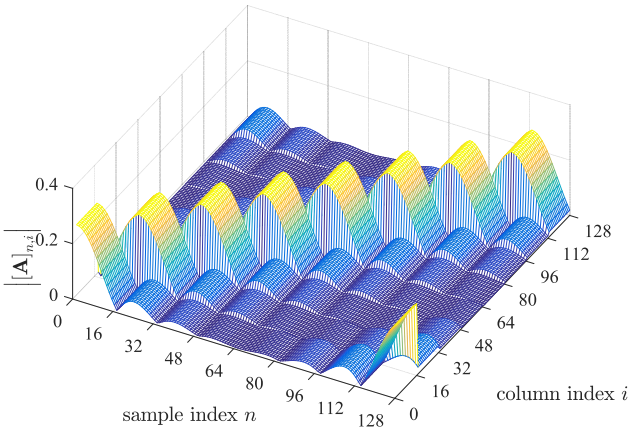

FIGURE 3. The time-frequency spectrograph of the GFDM system with $K = 16$, $M = 8$, and RC filter with roll-off factor $\alpha = 0.1$ is adopted.

and

$$\tilde{\mathbf{H}} = \begin{bmatrix} h_1 & & & & \\ h_2 & h_1 & & & \\ \vdots & h_2 & h_1 & & \\ h_{N_{ch}} & \vdots & h_2 & \ddots & \\ & h_{N_{ch}} & \vdots & \ddots & h_1 \\ & & h_{N_{ch}} & \vdots & h_2 \\ & & & \ddots & \vdots \\ & & & & h_{N_{ch}} \end{bmatrix}$$

stands for the $(N+N_{CP}+N_{ch}-1) \times (N+N_{CP})$ channel matrix which is convolution matrix with band-diagonal structure corresponding to the channel impulse response $\mathbf{h}$. At the receiver, under the assumption of perfect time and frequency synchronization, the signal model can be simplified after removing the CP as

$$\mathbf{y} = \mathbf{H}\mathbf{x} + \mathbf{z}, \qquad (6)$$

where $\mathbf{H}$ is the corresponding $N \times N$ circular convolution matrix. In particular, the matrix $\mathbf{H}$ would be simplified into an identity matrix when considering the AWGN channel and a diagonal matrix when the single-path Rayleigh channel is considered.

Step 5): After receiving $\mathbf{y}$, the linear MMSE receiver [7] is adopted to estimate the transmitted symbols as

$$\hat{\mathbf{d}} = \mathbf{B}_{MMSE}\mathbf{y}, \tag{7}$$

where $\hat{\mathbf{d}} = (\hat{d}_1, \hat{d}_2, \cdots, \hat{d}_N)$ and $\mathbf{B}_{MMSE} = \left(\mathbf{R}_z + (\mathbf{HA})^H(\mathbf{HA})\right)^{-1}(\mathbf{HA})^H$. Here, $\mathbf{R}_z$ denotes the covariance matrix of the noise $\tilde{\mathbf{z}}$.

Step 6): Finally, polar decoding can be carried out to recover the transmitted V bits.

III. CHANNEL POLARIZATION TRANSFORM

In this section, we introduce the idea of channel polarization into the GFDM modulation. The two-stage channel transform of PC-GFDM systems is presented, which consists of the GFDM channel transform and bit polarization transform. In the first stage, i.e., GFDM channel transform, sequential general modulation partition and parallel general modulation partition are considered, respectively. Their corresponding PC-GFDM systems are marked by MLC-PC-GFDM and BICM-PC-GFDM.

A. TWO-STAGE CHANNEL TRANSFORM FOR THE MLC-PC-GFDM SYSTEM

Assume quadrature amplitude modulation (QAM) with constellation modulation order J is adopted. Given the system model (6), suppose an ideal channel estimation is used in the receiver, i.e., the channel gain matrix $\mathbf{H}$ is known by the receiver. Let $W : \mathcal{X} \mapsto \mathcal{Y}$ denote the GFDM channel, where $\mathcal{X}$ is the set of transmitted vectors $\mathbf{x} = (x_1, x_2, \cdots, x_N)$ in (4) with $|\mathcal{X}| = 2^{JN}$, and $\mathcal{Y}$ is the set of received vectors $\mathbf{y}$. We use $W(\mathbf{y}|\mathbf{x}, \mathbf{H})$ to denote the transition probability, where $\mathbf{x} \in \mathcal{X}, \mathbf{y} \in \mathcal{Y}$. Given the constellation mapper and the GFDM modulation matrix $\mathbf{A}$, a JN-bit vector $\mathbf{b}$ is mapped into a waveform signal vector $\mathbf{x} \in \mathcal{X}$ under a definite one-to-one mapping $\mathcal{M}$,

$$\mathcal{M} : \mathbf{b} = (\mathbf{b}_1, \mathbf{b}_2, \cdots, \mathbf{b}_N) \in \mathbb{B}^{JN} \mapsto \mathbf{x} \in \mathcal{X}, \tag{8}$$

where $\mathbf{b}_n = (b_{n,1}, b_{n,2}, \cdots, b_{n,J}) \in \mathbb{B}^J, n = 1, 2, \cdots, N$ and $\mathcal{M}$ is called the generalized modulation mapping, where the QAM constellation modulation and the GFDM modulation can be regarded as a joint process of modulation. Therefore, the GFDM channel W is equivalently expressed as $W : \mathbb{B}^{JN} \mapsto \mathcal{Y}$, whose transition probability is

$$W(\mathbf{y}|\mathbf{b}, \mathbf{H}) = W(\mathbf{y}|\mathcal{M}^{-1}(\mathbf{x}), \mathbf{H}), \tag{9}$$

where $\mathcal{M}^{-1}(\cdot)$ is the inverse mapping of $\mathcal{M}$.

Since a JN-bit vector $\mathbf{b}$ is mapped into a waveform signal vector $\mathbf{x} \in \mathcal{X}$ through $\mathcal{M}$, the J-bit vector $\mathbf{b}_n$ is mapped into a signal point of the waveform space. Let $\mathcal{B} \subset \mathbb{B}^J$ denote the set of $\mathbf{b}_n$, the vector-input GFDM channel W is then decomposed into N channels $W_n : \mathcal{B} \mapsto \mathcal{Y}$, where $n = 1, 2, \cdots, N$. The transition probabilities of W_n can be written as

$$W_n(\mathbf{y}|\mathbf{b}_n) = \sum_{(\mathbf{b}\backslash\mathbf{b}_n)\in\mathbb{B}^{J(N-1)}} \frac{1}{2^{J(N-1)}} \cdot W(\mathbf{y}|\mathbf{b}). \tag{10}$$

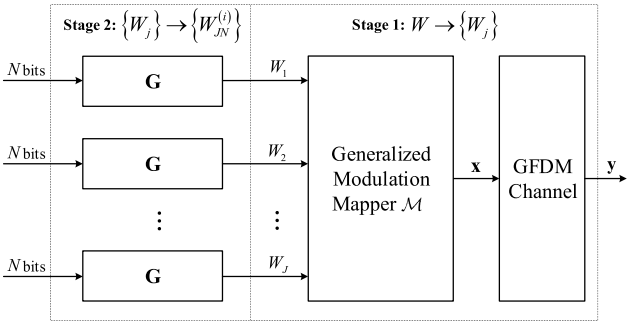

FIGURE 4. A diagram of the two-stage channel transform of the proposed MLC-PC-GFDM system.

where the notation $\mathbf{b}\backslash\mathbf{b}_n$ denotes a subvector of $\mathbf{b}$ with $\mathbf{b}_n$ excluded.

For the MLC-PC-GFDM system, based on the capacity properties of $\{W_n\}$ depicted in Section IV-A, we assume the N channels $W_n : \mathcal{B} \mapsto \mathcal{Y}, n = 1, 2, \cdots, N$ are independent with each other. Hence we neglect the index of sample and consider the channel $\bar{W} : \mathcal{B} \mapsto \mathcal{Y}$. Then through the two-stage channel transform depicted in Fig. 4, the channel $\bar{W}$ is divided into a series of bit polarized channels. In the first stage channel transform, the sequential general modulation partition is performed based on the MLC scheme in [2], then the bit polarization transform is utilized in the second stage channel transform.

Stage 1) Sequential general modulation partition: By regarding the generalized modulation mapping process $\mathcal{M}$ as a special kind of channel transform and based on the MLC scheme, the channel $\bar{W}$ can be decomposed into J synthesized BMCs $W_j : \mathbb{B} \mapsto \mathcal{Y} \times \mathbb{B}^{j-1}$, where $j = 1, 2, \cdots, J$, which are referred as GFDM synthesized channels. The transition probability of W_j are

$$W_j\left(\mathbf{y}, \mathbf{b}_{n,1:j-1}|b_{n,j}\right) = \sum_{\mathbf{b}_{n,j+1:J}\in\mathbb{B}^{J-j}} \frac{1}{2^{(J-1)}} \cdot W(\mathbf{y}|\mathbf{b}_n), \tag{11}$$

where $\mathbf{b}_{n,1:j-1}$ denotes a subvector of $\mathbf{b}_n$ that contains the first $j-1$ elements and $\mathbf{b}_{n,j+1:J}$ is a subvector of $\mathbf{b}_n$ that contains the last $J-j$ elements.

Stage 2) Bit polarization transform: In this stage, by performing the conventional N-dimensional channel polarization transform $\mathbf{G}_N$ [1] on each of these J synthesized channels W_j, a total of JN polarized BMCs $\{W_{JN}^{(i)}\}$ will be obtained, where $i = 1, 2, \cdots, JN$. The resulting BMCs are named as the bit polarized channels.

B. TWO-STAGE CHANNEL TRANSFORM FOR THE BICM-PC-GFDM SYSTEM

Based on the two-stage channel transform of the MLC-PC-GFDM system, the optimal performance can be achieved by using a multi-stage decoding (MSD) in the receiver, where the reliability values (e.g., LLRs) corresponding to the first bit level is computed first, which is passed to the first decoder. Then the decoding results will be used for the decoding of the

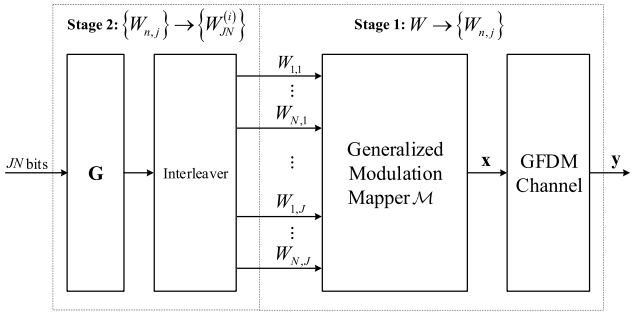

FIGURE 5. A diagram of the two-stage channel transform of the proposed BICM-PC-GFDM system.

next bit level, and so on. In contrast to the successive approach used for MLC-PC-GFDM with MSD, all bit levels are treated equally at both sides in the BICM-PC-GFDM system. At the transmitter, the source bits in BICM-PC-GFDM are encoded using a single polar encoder while at the receiver, parallel decoding is performed, where the relations between the bit levels are neglected and the reliability values are computed independently for each bit level based on the received signal. Finally, these bit metrics are then deinterleaved and fed together to the decoder.

Therefore, different from that of the MLC-PC-GFDM system, the two-stage channel transform of the BICM-PC-GFDM system is shown in Fig. 5, where the parallel general modulation partition is performed in the first stage channel transform based on the BICM scheme in [2]. Then the bit polarization transform is used in the second stage.

Stage 1) Parallel general modulation partition: As shown in (10), the vector-input GFDM channel W has been split into N channels $W_n : \mathcal{B} \mapsto \mathcal{Y}$, where $n = 1, 2, \cdots, N$. Then with the help of interleaver and under the assumption that the inputs of W_n are uniformly distributed, each 2^J-ary input channel W_n is further decomposed into J parallel independent BMCs, whose transition probabilities are expressed as

$$W_{n,j}\left(\mathbf{y}|b_{n,j}\right) = \sum_{(\mathbf{b}_n \backslash b_{n,j}) \in \mathbb{B}^{J-1}} \frac{1}{2^{J-1}} \cdot W_n\left(\mathbf{y}|\mathbf{b}_n\right), \quad (12)$$

where $j = 1, 2, \cdots, J$ and $\mathbf{b}_n \backslash b_{n,j}$ denotes a subvector of $\mathbf{b}_n$ with $b_{n,j}$ excluded. Note that the interleaver plays a crucial role in fading channels to ensure the consecutive coded bits to be affected by independent fades.

Thus, the GFDM channel W has been decomposed into a series of parallel BMCs $\{W_{n,j}\}$ in this stage, where $n = 1, 2, \cdots, N$ and $j = 1, 2, \cdots, J$, which are referred as the GFDM synthesized channels.

Stage 2) Bit polarization transform: In this stage, the binary-input JN-dimensional channel polarization transform denoted by $\mathbf{G}_{JN}$ is performed on the parallel GFDM synthesized channels $\{W_{n,j}\}$ to obtain JN polarized BMCs $\{W_{JN}^{(i)}\}$, where $i = 1, 2, \cdots, JN$, which are named as the bit polarized channels.

IV. PRACTICAL IMPLEMENTATION OF PC-GFDM SYSTEMS

In this section, we give the detailed construction procedure of the proposed PC-GFDM systems. The reliabilities of the two-stage polarized channels $\{W_{JN}^{(i)}\}$ are calculated for MLC-PC-GFDM and BICM-PC-GFDM, respectively.

A. THE CONSTRUCTION OF MLC-PC-GFDM

Recall (7), the linear MMSE receiver is employed to obtain the estimation $\hat{d}_n$ for the n-th transmitted symbol. Due to the subcarrier filtering existing in the GFDM modulation, $\hat{d}_n$ is interfered with the rest of symbols as

$$\hat{d}_n = \mathbf{C}_{n,n} d_n + \sum_{i=1, i\neq n}^{N} \mathbf{C}_{n,i} d_i + \sum_{i=1}^{N} \mathbf{B}_{n,i} z_i, \quad (13)$$

where $\mathbf{B} = (\mathbf{R}_z + \mathbf{A}^H\mathbf{A})^{-1}\mathbf{A}^H$ under AWGN channel, $\mathbf{C} = \mathbf{BA}$, d_n is the n-th transmitted symbol, the term $\sum_{i=1,i\neq n}^{N} \mathbf{C}_{n,i} d_i$ denotes the interference introduced by all other symbols and $\sum_{i=1}^{N} \mathbf{B}_{n,i} z_i$ stands for the corresponding noise. Hence, the signal to interference plus noise power ratio (SINR) corresponding to $\hat{d}_n$ can be derived as

$$SINR_n = \frac{\left\|\mathbf{C}_{n,n}\right\|^2 E_s}{\left(\sum_{i=1,i\neq n}^{N} \left\|\mathbf{C}_{n,i}\right\|^2\right) E_s + \left(\sum_{i=1}^{N} \left\|\mathbf{B}_{n,i}\right\|^2\right) N_0}, \quad (14)$$

where E_s denotes the average power of the transmitted symbols and N_0 represents the average power of the noise. According to the relationship between SINR and mean square error (MSE) under the linear MMSE receiver given in [9] [see Equ. (7)-(11)] and the structure of the GFDM modulation matrix $\mathbf{A}$, we have the following theorem.

Theorem 1: The capacities of channels $W_n : \mathcal{B} \mapsto \mathcal{Y}$, $n = 1, 2, \cdots, N$ are identical.

Proof: First, the capacity of W_n is determined by the SINR corresponding to the estimated symbol $\hat{d}_n$, hence to prove the theorem is equivalent to prove all the $SINR_n$ for $n = 1, 2, \cdots, N$ are identical. Then according to [9], the SINR corresponding to $\hat{d}_n$ can be related to the MSE of $\hat{d}_n$ as

$$SINR_n = \frac{1}{MSE_n} - 1, \quad (15)$$

and

$$MSE_n = \left[\left(\mathbf{I}_N + \mathbf{A}^H \mathbf{R}_z^{-1} \mathbf{A}\right)^{-1}\right]_{n,n}, \quad (16)$$

where $\mathbf{I}_N$ is the $N \times N$ identity matrix and $\mathbf{R}_z^{-1}$ is the inverse matrix of the noise covariance matrix $\mathbf{R}_z = N_0\mathbf{I}_N$. Hence, $\mathbf{R}_z^{-1} = \frac{1}{N_0}\mathbf{I}_N$ and $\mathbf{A}^H\mathbf{R}_z^{-1}\mathbf{A} = \mathbf{R}_z^{-1}\mathbf{A}^H\mathbf{A}$.

Therefore, to prove the theorem is further equivalent to prove all the MSE_n for $n = 1, 2, \cdots, N$ are identical. Suppose the prototype filter $\mathbf{g} = \mathbf{g}_{0,0} = (g_0, g_1, \cdots, g_{N-1})^T$, which satisfies $\mathbf{g}^T\mathbf{g} = 1$. As shown in Fig. 2, each column of $\mathbf{A}$ is a time and frequency shifted version of the prototype filter $\mathbf{g}$. Hence, for each $\mathbf{g}_{k,m}$, $k = 0, 1, \cdots, K-1$ and $m = 0, 1, \cdots, M-1$, there exists $\mathbf{g}_{k,m}^H\mathbf{g}_{k,m} = 1$. In other words,

all the diagonal elements of $\mathbf{A}^H\mathbf{A}$ are equal to 1. In summary, it's easy to know that all the MSE_n, i.e., the diagonal elements of $\left[\left(\mathbf{I}_N + \mathbf{A}^H\mathbf{R}_z^{-1}\mathbf{A}\right)^{-1}\right]$ are identical. Thus we complete the proof. ■

Furthermore, when the single-path Rayleigh channel is considered, the MSE of $\hat{d}_n$ can be calculated as

$$\begin{aligned} MSE_n &= E\left(MSE_{\mathbf{H},n}\,|\mathbf{H}\right) \\ &= E\left[\left(\mathbf{I}_N + \mathbf{R}_z^{-1}\mathbf{A}^H\mathbf{H}^H\mathbf{H}\mathbf{A}\right)^{-1}\right]_{n,n}, \end{aligned} \tag{17}$$

where $E(\cdot)$ denotes the expectation, the channel response matrix $\mathbf{H}$ is a diagonal matrix and satisfies $E\left(\mathbf{H}^H\mathbf{H}\right) = \mathbf{I}_N$. Since $\mathbf{H}$ is common for calculating $\{MSE_n, n = 1, 2, \cdots, N\}$, it's straightforward to know that all the MSE_n for $n = 1, 2, \cdots, N$ are identical and thus Theorem 1 also holds under the single-path Rayleigh channel.

By Theorem 1, the process of construction can be simplified by assuming the N channels $W_n : \mathcal{B} \mapsto \mathcal{Y}$, $n = 1, 2, \cdots, N$ are independent with each other and just consider the 2^J-ary input channel $\bar{W} : \mathcal{B} \mapsto \mathcal{Y}$.

Therefore, based on the two-stage channel transform presented in Section III-A, the whole procedure for constructing the MLC-PC-GFDM system is described as the following two steps:

Step 1) Capacity calculation of GFDM synthesized channels: The 2^J-ary input channel $\bar{W}$ can be split into J correlated GFDM synthesized channels $\{W_j\}, j = 1, 2, \cdots, J$. The average mutual information (AMI) of the W_j can be calculated as

$$I(W_j) = \sum_{\mathbf{b}_{n,1:j}\in\mathbb{B}^j} \int_{\mathbb{R}}\int_{\mathbb{R}} \frac{1}{2^j} p\left(y\,|\mathbf{b}_{n,1:j}\right) \log \frac{p\left(y\,|\mathbf{b}_{n,1:j}\right)}{p\left(y\,|\mathbf{b}_{n,1:j-1}\right)} du dv, \tag{18}$$

where $u = \Re(y)$, $v = \Im(y)$.

After obtaining the capacities of GFDM synthesized channels, guided by the identical capacity approximation idea, the GFDM synthesized channels $\{W_j\}$ can be approximated by the binary-input AWGN (BI-AWGN) channels $\{\tilde{W}_j\}$ with equivalent capacities

$$I(W_j) = I(\tilde{W}_j), \tag{19}$$

where $I(\tilde{W}_j)$ is written as

$$I\left(\tilde{W}_j\right) = -\int_R p_j(y) \cdot \log p_j(y)\, dy - \frac{1}{2}\log 2\pi e\sigma_j^2, \tag{20}$$

and

$$p_j(y) = \frac{1}{2\sqrt{2\pi\sigma_j^2}}\left(\exp\left(\frac{-(y-1)^2}{2\sigma_j^2}\right) + \exp\left(\frac{-(y+1)^2}{2\sigma_j^2}\right)\right). \tag{21}$$

Hence, the noise variance σ_j^2 of the equivalent BI-AWGN channel $\tilde{W}_j$ can be calculated [10].

Step 2) Reliability calculation of bit polarized channels: By using the σ_j^2 calculated above, the conventional methods, such as density evolution (DE) [11] and Gaussian approximation (GA) [12] can be adopted to evaluate the reliabilities of the corresponding bit polarized channels $\{W_{JN}^{(i)}\}$. Finally, the V most reliable channels among $\{W_{JN}^{(i)}\}$ are selected to transmit the information bits according to the system model described in Section II-B, and the other $JN - V$ channels are used to transmit the frozen bits.

B. THE CONSTRUCTION OF BICM-PC-GFDM

Based on the two-stage channel transform presented in Section III-B, the GFDM channel has been decomposed into JN bit polarized channels, whose reliabilities can be evaluated by the following two steps.

Step 1) Capacity calculation of GFDM synthesized channels: First based on the SINR calculated in (14) , the refined soft-symbols can be obtained, which are then utilized to calculate the log-likelihood ratio (LLR) of each code bit as

$$\Lambda\left(b_{n,j}\right) = \ln\frac{P\left(b_{n,j}=0|\mathbf{y}\right)}{P\left(b_{n,j}=1|\mathbf{y}\right)}, \tag{22}$$

where $b_{n,j}$ denotes the j-th bit of the n-th transmitted symbol d_n. Let $B_{n,j}$ and $L_{n,j}$ denote the random variables corresponding to $b_{n,j}$ and its LLR $\Lambda\left(b_{n,j}\right)$, respectively. Then the probability distribution function (PDF) of $p(L_{n,j}|b_{n,j})$ is estimated by using the Monte-Carlo simulation, hence, the AMI between $B_{n,j}$ and $L_{n,j}$ can be calculated as

$$\begin{aligned} &I(W_{n,j}) \\ &= I\left(B_{n,j}; L_{n,j}\right) \\ &= \sum_{b_{n,j}\in\mathbb{B}} \int_{\mathbb{R}} p\left(l|b_{n,j}\right) p\left(b_{n,j}\right) \log \frac{p\left(l|b_{n,j}\right)}{\sum\limits_{b'_{n,j}\in\mathbb{B}} p\left(l|b'_{n,j}\right) p\left(b'_{n,j}\right)} dl. \end{aligned} \tag{23}$$

Then, the GFDM synthesized channels $\{W_{n,j}\}$ will also approximated by the BI-AWGN channels $\{\tilde{W}_{n,j}\}$ with equivalent capacities

$$I(W_{n,j}) = I(\tilde{W}_{n,j}), \tag{24}$$

and the noise variance $\sigma_{n,j}^2$ of $\tilde{W}_{n,j}$ can be evaluated.

Step 2) Reliability calculation of bit polarized channels: In analogy to the code construction (step 2) of the MLC-PC-GFDM, the reliabilities of bit polarized channels $\{W_{JN}^{(i)}\}$ will be evaluated by DE [11] or GA [12] method by using $\sigma_{k,j}^2$. Finally, the V most reliable channels among $\{W_{JN}^{(i)}\}$ are elected to transmit the information bits.

V. PERFORMANCE EVALUATION

In this section, the block error ratio (BLER) performance of PC-GFDM systems is analyzed via simulation. The number of transmitted symbols in each block is configured as $N = 128$, the code rate is $R = \frac{1}{2}$ and the shaping pulse used in GFDM is raised cosine (RC) with roll-off factor α. The modulation order J is chosen in $\{2, 4, 6\}$, which corresponds to QPSK, 16QAM and 64QAM, respectively.

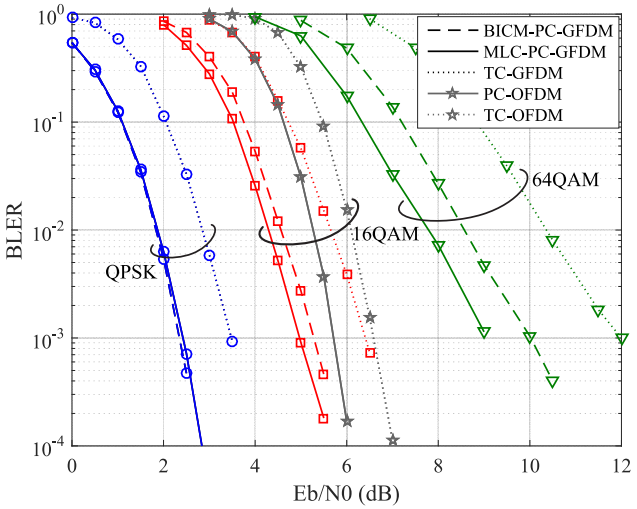

FIGURE 6. The BLER performances comparison among the proposed PC-GFDM systems and TC-GFDM system over AWGN channel, where $K = 16$, $M = 8$, $\alpha = 0.1$.

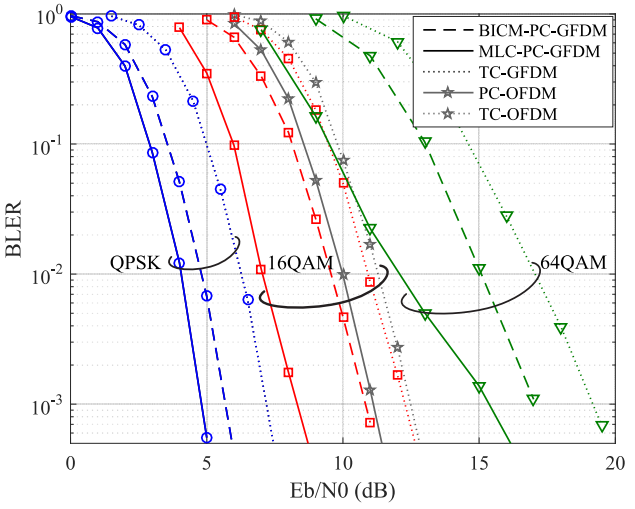

FIGURE 7. The BLER performances comparison among the proposed PC-GFDM systems and TC-GFDM system over single-path Rayleigh channel, where $K = 16$, $M = 8$, $\alpha = 0.1$.

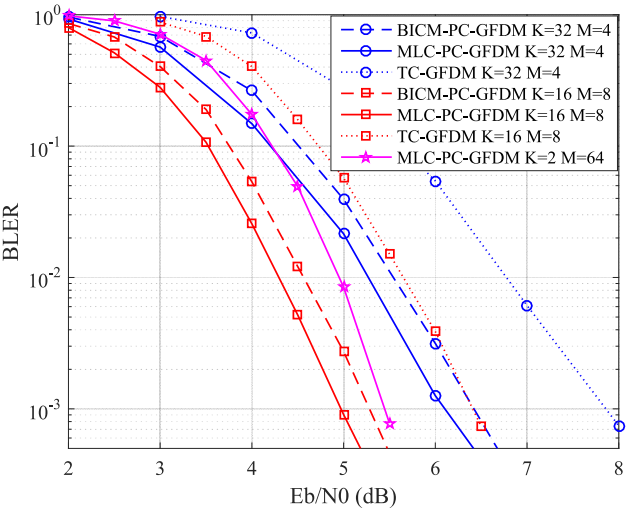

FIGURE 8. The BLER performances comparison under different configurations of K, M over AWGN channel, where $J = 4$ and $\alpha = 0.1$.

For comparison, the performances of turbo-coded GFDM (TC-GFDM) systems are also provided, where the turbo encoder and rate-matching algorithm adopted in the LTE system [13] are used, and the Log-MAP algorithm with maximum 8 iterations is used for turbo decoding. For polar codes, CRC aided adaptive SCL (aCA-SCL) [14] decoding algorithm with the maximum list size 32 is used. The simplified block interleaver proposed in [15] is employed in the BICM-PC-GFDM system. Further, the CRC-24 code in [13] is adopted for all coding schemes.

Fig. 6 compares the BLER performances of PC-GFDM systems and TC-GFDM system under AWGN channel, where the GFDM system is configured as $K = 16$, $M = 8$ and $\alpha = 0.1$. It can be observed that the proposed two PC-GFDM systems outperform the TC-GFDM system by $1 \sim 3$ dB for different modulation modes at the BLER of 10^{-3}, and the performance gain of PC-GFDM systems against TC-GFDM system becomes more obvious as the modulation order increases. Given the transmitted symbol length N, the higher modulation order means the larger code length. Hence, the above results essentially indicate the superiority of PC-GFDM schemes with long code length. Since the features of self-interference existing in GFDM transmitted symbols can be efficiently coordinated, PC-GFDM systems can achieve better performance than the TC-GFDM system. Besides, for the two proposed PC-GFDM systems, the BLER of MLC-PC-GFDM system achieves $0 \sim 1$ dB gain compared to that of the BICM-PC-GFDM system. When the modulation order $J = 4$ is adopted, the performances of PC-OFDM and TC-OFDM systems are also presented, which are slightly worse than those of the PC-GFDM and TC-GFDM systems.

Fig. 7 provides the BLER performances comparison among the PC-GFDM systems and TC-GFDM system under the single-path Rayleigh channel, where the system parameters are configured the same as those in Fig. 6. As shown in Fig. 7, the performance gain of the BICM-PC-GFDM system against the TC-GFDM system is about $1.5 \sim 2.2$ dB. What's more, the MLC-PC-GFDM system further outperforms the BICM-PC-GFDM system by about $0.9 \sim 2.5$ dB. Note that the performance gain in the situation of 64QAM is smaller than that in 16QAM because of the existence of rate matching.

Fig. 8 and Fig. 9 compare the BLER performances between PC-GFDM systems and TC-GFDM system with different system parameters configurations of K, M and α under AWGN channel. The modulation order is set to $J = 4$. It can be observed from Fig. 8 that distinct system performances emerge under the different configurations of K and M. The performance gain of PC-GFDM systems with $K = 16$, $M = 8$ against PC-GFDM systems with $K = 32$, $M = 4$ is about 1 dB as the BLER is 10^{-3}, while the performance gap of TC-GFDM systems even goes to 1.5 dB.

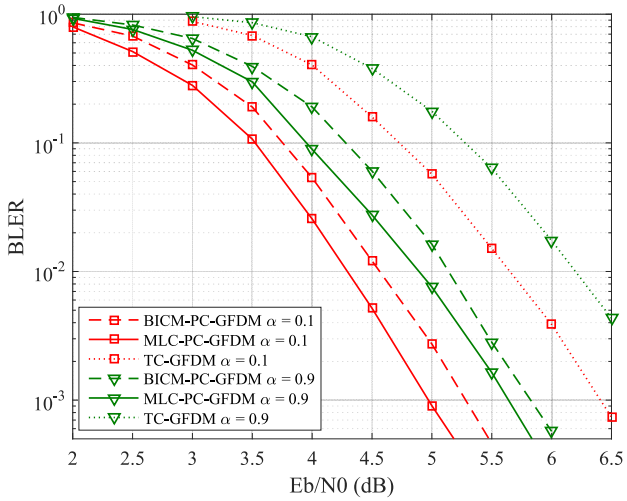

FIGURE 9. The BLER performances comparison under different α over AWGN channel, where $K = 16$, $M = 8$ and $J = 4$.

TABLE 1. The complexity comparison of PC-GFDM systems and TC-GFDM system.

Coded GFDM Systems	Encoding Complexity	Decoding Complexity
MLC-PC-GFDM	$JN \log N$	$\bar{L} \cdot JN \log N + 0.5 \cdot V \cdot 2\bar{L} \log\left(2\bar{L}\right)$
BICM-PC-GFDM	$JN \log JN$	$\bar{L} \cdot JN \log JN + 0.5 \cdot V \cdot 2\bar{L} \log\left(2\bar{L}\right)$
TC-GFDM	γN	$2 \cdot 4 \cdot 2^{\gamma} V I_t$

This is because different configurations of K and M can lead to distinct interference among transmitted symbols and thus affect the system performance to different degrees. However, no matter under which configuration of K and M, the MLC-PC-GFDM system always yields the best performance. Besides, as shown in Fig. 9, the adoption with $\alpha = 0.9$ of RC filter degrades both the performances of PC-GFDM systems and TC-GFDM system by approximate 0.5 dB, compared with that of $\alpha = 0.1$ situation. It confirms that the increase of roll-off factor will lead to more interference existing in the transmitted symbols, which degrades the system performance.

Finally, we analyze the encoding and decoding complexity of PC-GFDM systems and TC-GFDM system, which are listed in Table. 1. The decoding complexity of PC-GFDM systems with aCA-SCL [14] decoding consists of two parts, the computational complexity and the path selection complexity. The computational complexity for the BICM-PC-GFDM scheme is $\bar{L} \cdot JN \log JN$ and that is $\bar{L} \cdot JN \log N$ for the MLC-PC-GFDM scheme. And the path selection complexity for both PC-GFDM systems is $0.5 \cdot V \cdot 2\bar{L} \log\left(2\bar{L}\right)$, where $\bar{L}$ denotes the mean value of the list size and V is the length of information bits. According to [14], $\bar{L}$ is about 2 when the max size of list is 32 and BLER is 10^{-3}. For TC-GFDM system, since there are 2 component codes and 4 metric updating in each trellis node, the decoding complexity is $2 \cdot 4 \cdot 2^{\gamma} V I_t$, where I_t denotes the number of max iterations, and γ is the memory length of component code, which is 3 for LTE turbo code.

VI. CONCLUSION

In this paper, we establish a framework for the joint optimization of the binary polar coding and GFDM modulation. Based on the two-stage channel transform, we extend the channel polarization idea to the GFDM system, whereby the original GFDM channel is decomposed into a series of binary-input channels. Under this joint design framework, two practical PC-GFDM schemes are proposed, where the MLC-PC-GFDM scheme is designed to optimize the system performance, and the BICM-PC-GFDM scheme is proposed to reduce the processing latency and complexity. Simulation results indicate that the proposed PC-GFDM systems yield significantly better performance compared with the existing TC-GFDM system for different scenarios.

ACKNOWLEDGMENT

This article was presented in part at the 2017 IEEE International Symposium on Personal, Indoor and Mobile Radio Communications, Montreal, QC, Canada, October 2017.

REFERENCES

[1] E. Arıkan, "Channel polarization: A method for constructing capacity-achieving codes for symmetric binary-input memoryless channels," *IEEE Trans. Inf. Theory*, vol. 55, no. 7, pp. 3051–3073, Jul. 2009.
[2] M. Seidl, A. Schenk, C. Stierstorfer, and J. B. Huber, "Polar-coded modulation," *IEEE Trans. Commun.*, vol. 61, no. 10, pp. 4108–4119, Oct. 2013.
[3] G. Caire, G. Taricco, and E. Biglieri, "Bit-interleaved coded modulation," *IEEE Trans. Inf. Theory*, vol. 44, no. 3, pp. 927–946, May 1998.
[4] J. Dai, K. Niu, Z. Si, C. Dong, and J. Lin, "Polar-coded non-orthogonal multiple access," *IEEE Trans. Signal Process.*, vol. 66, no. 5, pp. 1374–1389, Mar. 2018.
[5] J. Dai, K. Niu, and J. Lin, "Polar-coded MIMO systems," *IEEE Trans. Veh. Technol.*, vol. 67, no. 7, pp. 6170–6184, Jul. 2018.
[6] G. Fettweis, M. Krondorf, and S. Bittner, "GFDM—Generalized frequency division multiplexing," in *Proc. IEEE 69th Veh. Technol. Conf.*, Barcelona, Spain, Apr. 2009, pp. 1–4.
[7] N. Michailow, M. Matthé, I. S. Gaspar, A. N. Caldevilla, L. L. Mendes, A. Festag, and G. Fettweis, "Generalized frequency division multiplexing for 5th generation cellular networks," *IEEE Trans. Commun.*, vol. 62, no. 9, pp. 3045–3061, Sep. 2014.
[8] G. R. Al-Juboori, A. Doufexi, and A. R. Nix, "System level 5G evaluation of GFDM waveforms in an LTE-A platform," in *Proc. IEEE ISWCS*, Poznan, Poland, Sep. 2016, pp. 335–340.
[9] D. P. Palomar, J. M. Cioffi, and M. A. Lagunas, "Joint Tx-Rx beamforming design for multicarrier MIMO channels: A unified framework for convex optimization," *IEEE Trans. Signal Process.*, vol. 51, no. 9, pp. 2381–2401, Sep. 2003.
[10] D. Zhou, K. Niu, and C. Dong, "Construction of polar codes in Rayleigh fading channel," *IEEE Commun. Lett.*, vol. 23, no. 3, pp. 402–405, Mar. 2019.
[11] R. Mori and T. Tanaka, "Performance of polar codes with the construction using density evolution," *IEEE Commun. Lett.*, vol. 13, no. 7, pp. 519–521, Jul. 2009.
[12] P. Trifonov, "Efficient design and decoding of polar codes," *IEEE Trans. Commun.*, vol. 60, no. 11, pp. 3221–3227, Nov. 2012.
[13] *Multiplexing Channel Coding, Release 12*, document TS 36.212, 3GPP, 2014. [Online]. Available: http://www.3gpp.org/ftp/Specs/2014-12/Rel12/36_series/
[14] B. Li, H. Shen, and D. Tse, "An adaptive successive cancellation list decoder for polar codes with cyclic redundancy check," *IEEE Commun. Lett.*, vol. 16, no. 12, pp. 2044–2047, Dec. 2012.
[15] Y. Li, J. Dai, K. Niu, and C. Dong, "Design of polar coding for GFDM system," in *Proc. IEEE 28th Annu. Int. Symp. Pers., Indoor, Mobile Radio Commun. (PIMRC)*, Oct. 2017, pp. 1–6.

YAN LI (S'17) received the B.S. degree in information engineering from the Beijing University of Posts and Telecommunications (BUPT), Beijing, China, in 2016, where she is currently pursuing the Ph.D. degree with the School of Information and Communication Engineering. Her research interests include information theory, coding theory, multicarrier modulation, and NOMA signal processing.

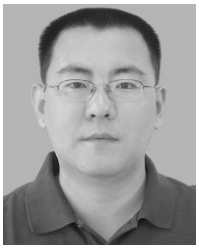

KAI NIU (M'12) received the B.S. degree in information engineering and the Ph.D. degree in signal and information processing from the Beijing University of Posts and Telecommunications (BUPT), Beijing, China, in 1998 and 2003, respectively, where he is currently a Professor with the School of Information and Communication Engineering. Since 2008, he has been a Senior Member with the Chinese Institute of Electronics and a Committee Member of the Information Theory Chapter, CIE. His research interests include coding theory and its applications, space-time codes, and broadband wireless communication. He is also an Associate Editor of the IEEE COMMUNICATIONS LETTERS.

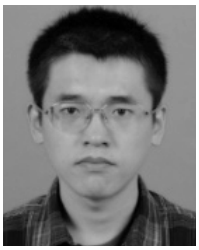

CHAO DONG (M'16) received the B.S. and Ph.D. degrees in signal and information processing from the Beijing University of Posts and Telecommunications (BUPT), Beijing, China, in 2007 and 2012, respectively, where he is currently an Associate Professor with the School of Information and Communication Engineering. His research interests include MIMO signal processing, multiuser precoding, decision feedback equalizer, and the relay signal processing.